Dynamic response of floating offshore renewable energy devices: Sensitivity to mooring rope stiffness

K. Smith, T. Davey, D. Forehand, A.C. Pillai, L. Tao, and Q. Xiao

***Abstract*—The offshore renewable energy sector has seen a rise in floating devices, all of which require mooring and anchoring systems. Synthetic ropes have emerged as a promising technology for cost reduction in this system. However, characterising the behaviour of these materials, which exhibit complex non-linear, visco- elastic and plastic structural properties, presents challenges. Numerical modelling and tank testing are the available tools for developers to overcome these challenges, however, there is a lack of guidelines for test facilities regarding the design of tank-scale mooring systems. The present work focuses on the numerical design of a typical semi-taut mooring system using synthetic materials suitable for future-generation floating offshore wind turbines. A coupled time-domain hydrodynamic model was employed to explore the dynamic sensitivity of the device to changes in mooring rope stiffness. The results demonstrate that changes in line axial stiffness have a greater impact on platform surge and mooring line tension than on heave and pitch responses. These findings establish preliminary margins for target stiffness values, which are valuable for selecting mooring materials for scaled tank test models. Although the case study was floating wind, the results have broader applicability to wider floating marine energy device design.**

***Index Terms*—tank testing, numerical modelling, synthetic moorings, floating offshore wind, taut mooring**

I. Introduction

OFFSHORE renewable energy (ORE), including wind, wave, and tidal technologies, plays a crucial role in the transition to net-zero. However, the high levelised cost of energy (LCOE) associated with ORE remains a barrier to commercial projects [1]. As such, cost reductions via design innovation are essential to achieve the deployment targets.

This paper is Submission #427 to Proceedings of the European Wave and Tidal Energy Conference 2023. The work was completed as part of the EPSRC and NERC Industrial Centre for Doctoral Training for Offshore Renewable Energy (IDCORE) which is funded by the EPSRC and NERC (EP/S023933/1).

K. Smith is undertaking their EngD research through IDCORE at the FloWave Ocean Energy Research Facility, University of Edinburgh, Edinburgh EH9 3BF, UK (e-mail: ka.smith@ed.ac.uk).

T. Davey is with the FloWave Ocean Energy Research Facility, University of Edinburgh, Edinburgh EH9 3BF, UK (e-mail: tom.davey@ed.ac.uk).

D. Forehand is with the School of Engineering, University of Edinburgh, Edinburgh EH9 3BF, UK (e-mail: d.forehand@ed.ac.uk).

A.C. Pillai is with the Renewable Energy Group, Department of Engineering, University of Exeter, Penryn TR10 9FE, UK (e-mail: a.pillai@exeter.ac.uk).

L. Tao and Q. Xiao are with the the Department of Naval Architecture, University of Strathclyde, Glasgow G1 1XQ, UK (e-mails: longbin.tao@strath.ac.uk, qing.xiao@strath.ac.uk).

Floating ORE devices, including floating wind farms (e.g., Hywind and Kincardine), wave devices (e.g., Mocean's BlueX and the AWS wave power buoy), and tidal turbines (e.g., Orbital Marine Power's O2), are gaining popularity in the sector [2]–[6]. The floating configuration offers advantages such as ease of maintenance, increased energy generation potential, and expanded deployment locations [7]. However, all floating systems require a mooring and anchoring system, which incurs significant capital and operational costs, up to 12% and 25% respectively for marine energy devices [8]–[10]. Reducing these costs has become a key research target.

Floating offshore wind turbines (FOWT)s, as the most mature marine renewable technology, initially adopted mooring designs from the oil and gas (O&G) industry. The prevalent multi-line chain catenary systems were chosen for their simplicity and ease of manufacture. This choice was appropriate in the early stages of floating wind to de-risk projects, however, catenary systems have drawbacks, including high fabrication and handling costs due to the need for large service vessels and colossal chain lengths [11]. Moreover, the design requirements for FOWTs differ from O&G platforms, necessitating optimised mooring designs specifically tailored for ORE applications [12]. Current research explores various aspects of mooring design optimisation, including alternative mooring types and configurations [11]–[13], arrangement and number of lines [14], materials and components [15]–[18], and anchor types [19].

In addition to technical innovation, increasing turbine capacity through economies of scale is another approach to reduce LCOE [20]. Leading turbine manufacturers are developing prototypes with ever higher ratings, predicted to reach 20+ MW models by the mid-2030s [21]. To facilitate collaboration between academia and industry, NREL and IEA introduced the IEA 15 MW offshore reference wind turbine (RWT) in 2020, serving as a benchmark for innovation [22]. Further to this, the University of Maine developed the VolturnUS-S, a semi-submersible floating platform designed specifically for the IEA 15 MW RWT [23]. These reference models have been widely adopted in studies investigating various aspects of offshore wind [16], [18]–[20], [24], [25].

This work focuses on semi-taut synthetic moorings as a means to reduce costs in the offshore renewable energy sector. The first part of the study employed a coupled numerical model to design a representative semi-taut mooring system for a large-scale 15 MW floating wind turbine in a typical environment. The second part addressed the challenge of scaling the mooring system for tank testing, particularly considering mooring stiffness. A numerical sensitivity analysis was conducted to investigate the impact of mooring line axial stiffness on the platform's dynamic behaviour. The findings from the sensitivity analysis provide estimates of uncertainty in dynamic results obtained from tank tests.

A. Semi-taut moorings

Synthetic materials offer favourable characteristics for offshore moorings, including high strength, compliance, low weight, and competitive cost [15], [16]. They have been used in O&G offshore moorings for decades and as such have attracted attention in the ORE sector. The academic literature can be categorised into state-of-the-art reviews exploring the potential of synthetic materials in ORE markets [13], [15], and studies developing numerical models for specific applications [11], [12], [16]. Various synthetic materials are available for offshore mooring configurations but polyester is the most widely accepted due to its good durability characteristics [13], [15], [21]. Notably, off-the-shelf polyester products suitable for permanent ORE moorings are currently available [26].

The structural properties of synthetic materials make them suitable for tensioned moorings, which rely on the elasticity of synthetic ropes to provide the platform's restoring moment. Semi-taut moorings, a type of tensioned mooring, can be seen as a hybrid between spread taut moorings and catenary moorings. While lacking a formal definition, semi-taut lines generally consist of a tensioned rope segment, creating a distorted catenary shape, followed by a section of free-hanging heavy anchor chain. This design yields lighter and shorter lines compared to plain catenary moorings, providing cost advantages for shallower and deeper water systems [13]. Furthermore, tensioned moorings increase platform stability, leading to greater power generation [1], and reduce the seabed footprint, thereby mitigating negative ecological impact [27]. As such, market projections on the mooring and anchoring systems of FOWTs by ORE Catapult predict that buoyant semi-taut moorings will dominate after 2030 as deployments accelerate [21]. At present, industry has seen several floating energy demonstrators and projects deploying tensioned moorings using sections of synthetic material [15]. However, modelling the structural and fatigue properties of synthetic ropes in the irregular offshore environment is challenging due to their non-linear and time-dependent load-extension response [12], [15]. While tank testing has historically been a tool to validate complex numerical modelling, minimal published work focuses on the physical modelling of scaled synthetic moorings for tank testing.

B. Modelling mooring stiffness

The load-extension response of a line is crucial in semi-taut mooring design, as the line's axial stiffness impacts the system's compliance. A finite element lumped mass model was utilised to represent the mooring line and is well-explained by Borg et al. [28]. In summary, the mooring line is discretised into massless spring-damper segments connected at nodes, where the total forces and moments are summed. Of the various stiffness properties (axial, bending, and torsional), axial stiffness holds the greatest influence in terms of its order of magnitude. It is obtained by the gradient of the material's load-extension graph at an instantaneous strain. The tension force of the line is a function of the axial stiffness, which in itself is a function of the applied load and thus displacement. Hysteresis in axial stiffness, a characteristic of synthetic ropes, was not considered in this study but should be investigated in future research.

C. Design of tank-scale mooring systems

International standards like ISO 19901-7, API RP 2SK, and DNV-OS-J103 [29]–[31] promote the use of model tests to validate numerical models for station-keeping systems. DNV-OS-J103, specifically written for floating wind systems, advises using accurately scaled mooring systems or soft moorings with springs for testing. When using a soft system, it recommends selecting spring stiffness to ensure realistic natural frequencies. However, there is no specific guidance on the design of accurately scaled moorings other than aiming for geometric and structural similitude.

The design of mooring systems for tank-scale testing poses various scaling challenges. Tank dimensions can limit mooring geometry, i.e, line length, water depth and spread, but methods like using truncated lines and altering angles can partially overcome this [32], [33]. Constructing scaled prototypes for testing raises further challenges in accurately scaling line axial stiffness using ropes and/or springs. Froude scaling, which scales axial stiffness by a factor of λ^3, is commonly used in hydrodynamic testing [8]. However, it has been observed that tank model mooring stiffness is often much greater than the equivalent scaled value of the full-scale device [33]–[35]. The present paper aims to explore methods for quantifying the uncertainty in tank model results when using crudely scaled line stiffness values.

D. Paper layout

This paper includes: Section II (numerical modelling approach, case-study definition, and sensitivity study), Section III (presentation of results), Section IV (further exploration of findings), and Section V (conclusions).

II. Methodology

OrcaFlex [36] was utilised for all numerical analysis. For this model, a semi-taut mooring system was designed for a 15 MW floating wind turbine supported

by a semi-submersible platform. A sensitivity analysis was conducted using this model to assess the impact of changes to the line axial stiffness on model dynamics.

A. Numerical model

OrcaFlex is a commercial tool for fully-coupled hydrodynamic analysis and is widely used in the floating wind industry. It has been extensively validated [37] against other hydrodynamic software, physical testing results and analytical calculations.

The environmental conditions for the case-study design load cases were obtained using various methods. TurbSim [38], a turbulent-wind simulator, was used to define the wind input with a Kaimal wind turbulence spectrum [39]. Irregular waves were generated in OrcaFlex using JONSWAP spectral parameters [39]. Identical seeds were used for repeatability. Simulations had a start-up ramp period, and the simulation lengths were 3600 s for final design iterations and 600 s for the stiffness sensitivity study, following the IEC 61400-3-2 standard [40]. Periodic 2D wind simulations of 600 s were repeated over the full simulation length wave series to create the full loading condition.

B. Design of a typical semi-taut mooring

This section defines the case-study environmental conditions, balance of plant, and mooring system.

1) Environmental conditions: The selected environmental conditions represent the east coast of the US with a water depth of 200 m, based on the original platform definition [23]. For design qualification, the standards specify a set of design load cases (DLC)s which encompass various combined environmental loading conditions, directions, probabilities, and turbine statuses. For ultimate limit state analysis, the DNV-OS-J103 standard [31] recommends modelling a minimum of two cases.

The first case, DLC 1.1, represents the power production condition with applied sustained wind speeds within the turbine's operating range. The second case, DLC 1.6, also represents power production but with maximum operable wind speeds to provide a baseline for the ultimate limit state analysis. The third and final case, DLC 6.1, represents a 50-year extreme environmental loading event, where the turbine is parked and thus the aerodynamic load reduced. Table I provides wind and wave parameters for the chosen DLCs. No environmental misalignment or current was modelled.

2) Balance of plant: The turbine selected for this study is the IEA 15 MW RWT [22]. This large-capacity turbine serves as a relevant benchmark for the advancement of next-generation FOWTs. The chosen platform is the VolturnUS-S reference semi-submersible platform [23]. The platform design closely resembles existing commercial models, providing a realistic basis for the study.

3) Mooring system definition: The catenary mooring system defined in the definition of the VolturnUS-S reference platform [23] provided the baseline design of the alternative semi-taut system. The original mooring consists of three 850 m long, 185 mm diameter R3 studless chains spaced radially at 120°. However, both the document and market projections suggest that a smaller chain size would be sufficient and more aligned with industry expectations [21]. Therefore, the baseline catenary mooring was updated to utilized a 152 mm diameter R3 chain to avoid over-engineering and better match market trends.

The minimum breaking load (MBL) of the catenary chain was matched with the MBL of the synthetic rope to identify the equivalent synthetic rope diameter, an approach taken in a study by Pillai et al. [16]. Accordingly, the 234 mm Bridon MoorLine Polyester rope was chosen, which aligned with market projections of polyester rope diameters around 230 mm [21]. The selected rope had a MBL of 15696 kN and its stiffness profile is shown in Fig. 1 with the caveat that it had an almost linear axial stiffness, with non-linear deviations only at low strains. Whilst uncharacteristic of synthetic materials, this rope choice was still in-keeping with industrial trends.

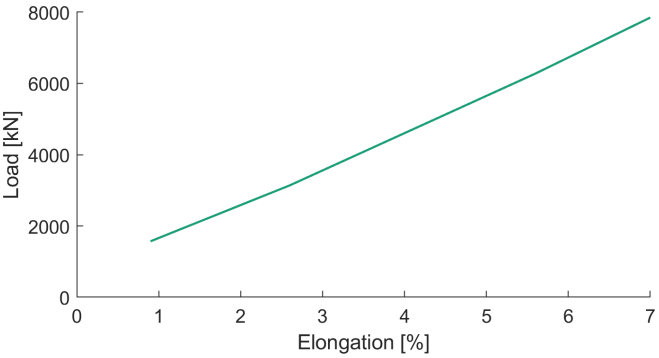

Fig. 1: Bridon MoorLine Polyester load-extension [26]

Each mooring line followed a chain-rope-chain construction as specified in ISO 19901-7. The fairlead and anchor chain lengths were chosen in line with similar studies and were not optimised further [11], [13], [16]. This configuration protects the synthetic rope from UV damage near the water surface and minimises exposure to the abrasive seabed environment. 152 mm R3 chain was used at the fairlead and anchor attachments. The mooring line angle with the seabed for semi-taut FOWT mooring systems is typically between 30-45° [13], however, shallower angles can be achieved in shallower water depths [11], [16]. This work will initially employ an angle of 45° to minimise line length and therefore associated procurement and installation costs. Minimising anchor loads was not within the scope of this study.

The semi-taut mooring design was generated based on the design criteria listed below. An iterative process was used to vary pretension by modifying the synthetic section length, and mooring line angle. The pretensions

TABLE I: Design load cases (DLC)s and environmental parameters. NTM = Normal Turbulence Wind Model, EWM = Extreme Wind Speed Model, NSS = Normal Sea State, SSS = Severe Sea State, ESS = Extreme Sea State. [Adapted from [23]]

DLC	Wind condition	Hub height wind speed [m/s]	Wind direction [°]	Sea state	Significant wave height (H_S) [m]	Mean zero-crossing period (T_Z) [s]	Wave direction [°]
1.1	NTM	24	0	NSS	4.52	7.02	0
1.6	NTM	24	0	SSS	9.80	10.80	0
6.1	EWM	38	0	ESS	10.70	10.87	0

were achieved by observing zero heave displacement with the original platform ballast [23].

1) Limit platform translation to 25 m in order to avoid damage to the electrical umbilical cable as specified in the original documentation [23]
2) Limit maximum pretension to 3000 kN to ensure feasibility of marine operations [21]
3) Limit minimum line tension to above 2% MBL to avoid snatch loads [11]
4) Limit peak tension loads to 60% MBL with a safety factor of 1.67 in accordance with ISO 19901-7 [29], assuming a redundant mooring.

C. Axial stiffness sensitivity study

Scaling the material properties accurately for prototype testing can be challenging. Accordingly, a sensitivity analysis was performed to evaluate the dynamic response of the entire system to variations in individual mooring line axial stiffness. A spectrum of mooring line axial stiffness values were analysed to establish a range of values suitable for scaling down to the prototype model with confidence.

As explained in Section I-B, axial stiffness is directly proportional to the elongation of a specimen under a given load. To generate the range of stiffness profiles, the elongations provided in the data sheet of Bridon MoorLine polyester rope [26] were multiplied by a set of factors. A total of 10 multiplication factors were chosen, consistent with the triangular number sequence. This gave a total of 20 stiffness values, 10 of increased stiffness and 10 decreased stiffness. The range of stiffness profiles is shown in Fig. 2. All profiles were based on the original baseline profile of the Bridon MoorLine rope, following the same stiffness regime. It should be noted that in reality, ropes with different compliance characteristics may exhibit distinct non-linear profiles.

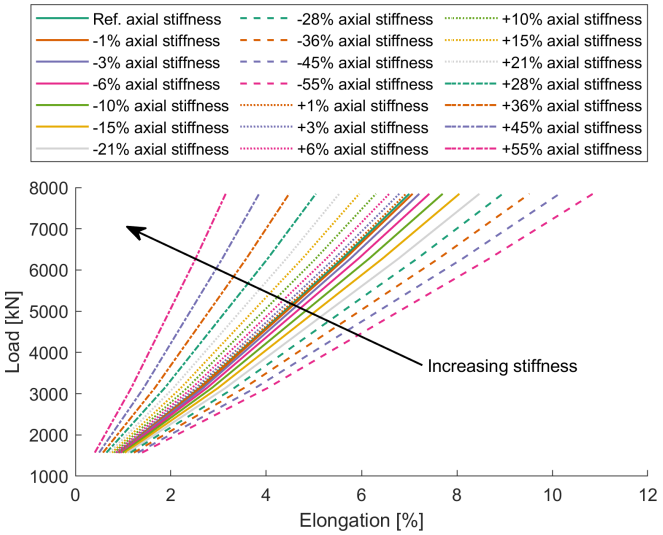

Fig. 2: Mooring rope non-linear axial stiffness profiles for sensitivity study

D. Summary of simulations

Table II describes the simulations for the semi-taut mooring design and stiffness sensitivity analysis.

TABLE II: Summary of simulations

Scheme	Axial stiffness [% Ref. [a]]	Sim. length [s]	# seeds	DLC		
				1.1	1.6	6.1
Design of semi-taut mooring	Ref.	3600	3 [b]	✓	✓	✓
Axial stiffness sensitivity	[-55 -45 -36 -28 -21 -15 -10 -6 -3 -1 Ref. +1 +3 +6 +10 +15 +21 +28 +36 +45 +55]	600	1	✓	✓	✓

[a] The reference mooring line axial stiffness refers to the load-extension profile provided in the Bridon MoorLine Polyester datasheet [26].
[b] Three seeds were considered for the severe and extreme DLCs 1.6 and 6.1. Only one seed was considered for the normal DLC 1.1 as this work was a conceptual study [40].

III. Results

The results of both parts of this study as listed in Table II are presented, including platform motion and line tension. Box and whisker plots were selected as they allow direct comparison between different models and the design criteria. The statistical distribution of data is represented by the height of the box showing the interquartile range, the whiskers extending to the maximum and minimum values, and any outliers are shown as singularities beyond this. The data median is at the horizontal line in the box and the mean has been plotted as a black circle. One limitation of using box and whisker plots is their inability to capture information regarding changes in the phase of the dynamic response.

A. Semi-taut mooring design: Reference axial stiffness

A semi-taut mooring system for the IEA 15 MW RWT and VolturnUS-S platform was developed using Bridon MoorLine polyester rope. A set of limiting design specifications was defined to establish the preliminary performance of the system. Fig. 3 shows the geometry and numbering of the resulting mooring system.

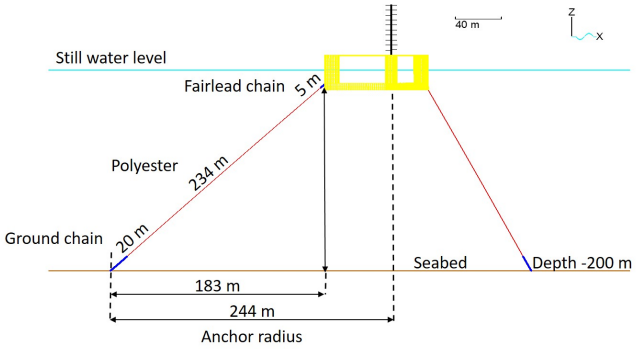

(a) Details of mooring line geometry

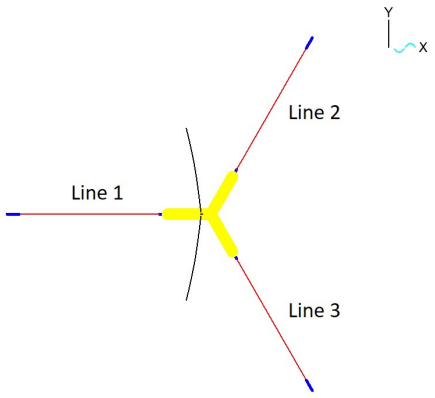

(b) Plan view of model indicating line numbering

Fig. 3: OrcaFlex model of semi-taut mooring system

1) Platform motions: The platform motion in surge, heave and pitch is shown in Fig. 4. The maximum surge was observed under the severe DLC 1.6. This result highlighted the importance of considering different loading schemes in the ultimate limit state analysis. The maximum heave displacement and pitch rotations were observed under extreme DLC 6.1.

TABLE III: Maximum platform motions for all DLCs

DLC	Platform motion		
	Surge [m]	Heave [m]	Pitch [°]
1.1	4.61	1.30	-3.21
1.6	8.43	4.31	-4.05
6.1	8.14	4.66	-4.07

2) Mooring line loads: A pretension of 2350 kN, equivalent to 15% MBL, was observed in each line. In addition, the line tension loads for all three DLCs are shown in Fig. 5. The tensions are normalised to the rope's MBL. The highest loads were present in line 1 under the extreme DLC 6.1. The bulk statistics show the loading in lines 2 and 3 are similar, which is as expected for a symmetrical mooring spread. For the severe and extreme DLC, there are outlier points indicating potential slack line events and breach of the design loading criteria. It should be noted that this minimum tension breach only occurred in one seed condition, highlighting the importance of simulating multiple seeds to fully quantify the system's response. A time series of one such extreme event is shown in Fig. 6. This series shows the tension in line 3 under DLC 6.1 dropping to 1.7% MBL and then rapidly increasing to 20.3% MBL. Table IV shows the numerical values of the maximum and minimum tensions in each line for each DLC and compares the results against the design criteria, highlighting the slack line event.

TABLE IV: Maximum and minimum tension loads in each line under all DLCs compared with design criteria

DLC	Normalised tension [% MBL]				Criteria fulfilled?
	Criteria	Line 1	Line 2	Line 3	
1.1	Max $<$ 60	24.4	17.3	17.5	✓
1.6		35.6	24.0	24.3	✓
6.1		36.8	25.2	25.8	✓
1.1	Min $>$ 2	12.8	9.8	9.6	✓
1.6		6.7	3.7	2.7	✓
6.1		6.8	2.8	1.7	X

3) Design criteria assessment: Four design limitations on maximum platform motions and mooring line tensions were established to assess the performance of the novel semi-taut mooring system. Table V summarises the fulfillment of these criteria. The highlighted row represents the slack line event, which breached the minimum line tension design criteria. For this study, meeting the other three criteria was deemed acceptable, as the mooring design was not intended as a final, installation-ready design but rather to reflect current industry trends. In practice, if slack line events were observed during the mooring design process, the lines' pretension would be increased, and the platform re-ballasted. However, altering the original platform specification was beyond the scope of this work.

TABLE V: Design criteria assessment

#	Description	Limit value	Design value	Fufilled?
1	Max. motion	25 m	8.43 m	✓
2	Pretension	3000 kN	2350 kN	✓
3	Min. tension	2% MBL	1.7% MBL	X
4	Max. tension	60% MBL	36.8% MBL	✓

B. Axial stiffness sensitivity results

The axial stiffness sensitivity was analysed using identical semi-taut design parameters and DLCs as in the first part of this study.

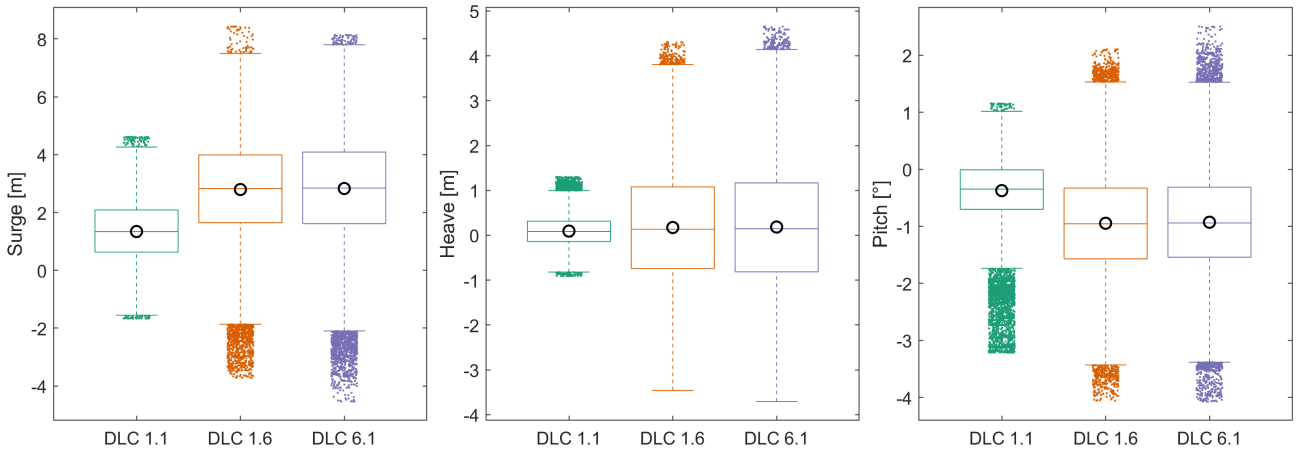

Fig. 4: Statistical comparison of platform motions in surge, heave and pitch degrees of freedom for each DLC. These results reflect the mooring design with reference line axial stiffness.

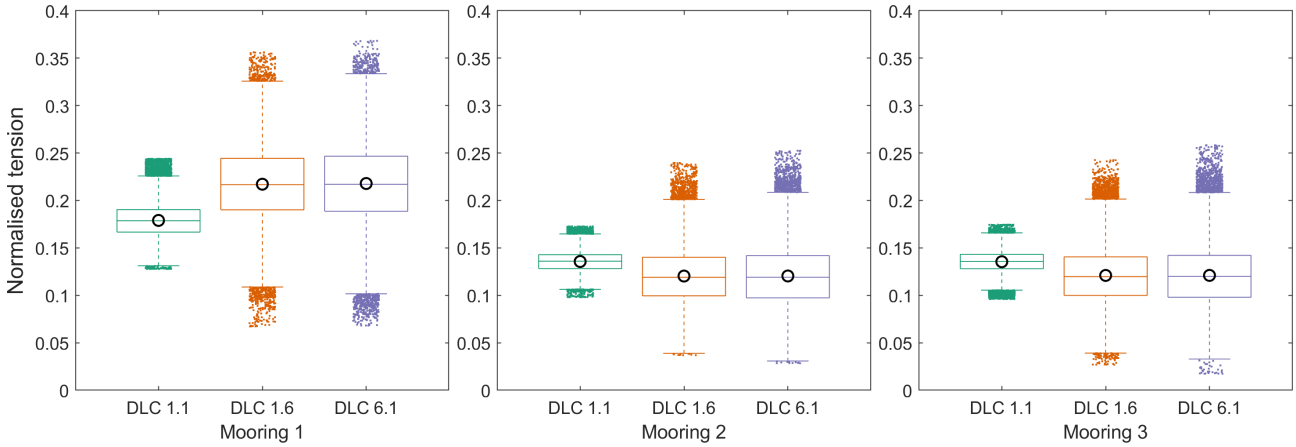

Fig. 5: Statistical comparison of normalised mooring line loads for each line under each DLC. These results reflect the mooring design with reference line axial stiffness.

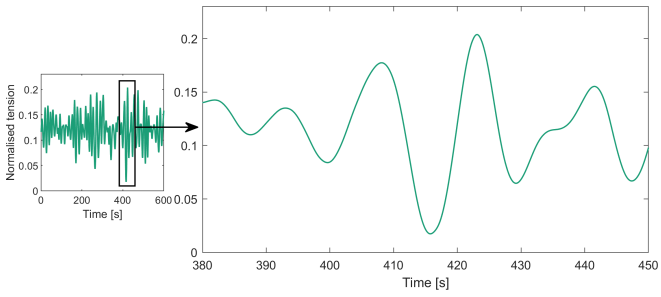

Fig. 6: Potential snatch loading event on mooring 3 in DLC 6.1 (seed 3)

1) Platform motions: The statistical distribution of the platform displacements is shown in Figure 7. Each row in the figure represents a single degree of freedom, while each column corresponds to a specific DLC. The analysis reveals that surge is the most sensitive to variations in line axial stiffness. Reductions in stiffness lead to increased surge mean values and amplitudes, and vice versa. This relationship is more pronounced in the extreme DLC 6.1 compared to the normal DLC 1.1. Conversely, the mean heave displacement is only sensitive to increases in line axial stiffness which is likely an offset from the static position. In reality this would be compensated by increasing line length for stiffer materials. Changes in line axial stiffness appear to have no significant impact on mean pitch values across all DLCs.

2) Mooring line loads: A comparison of mooring tensions is shown in Figure 8. Each row is a single mooring line, and each column a DLC. Increasing the line's axial stiffness leads to an increase in the mean mooring tension, and vice versa. This relationship is consistent for all lines and DLCs.

3) Implications for tank test mooring design: To apply the sensitivity analysis to tank mooring design, the motion and tension results were compared with those of the reference design. In this work, the term *uncertainty* represents the difference between these results, providing insights into potential uncertainties in tank results when using a mooring line with a different axial stiffness than the target value. To enable numerical comparisons and identify trends, the uncertainty limit was set to ±20% of the reference results. It's important to clarify that this value is not a physical quantity but allows quantifiable comparisons between line stiffness and system dynamics.

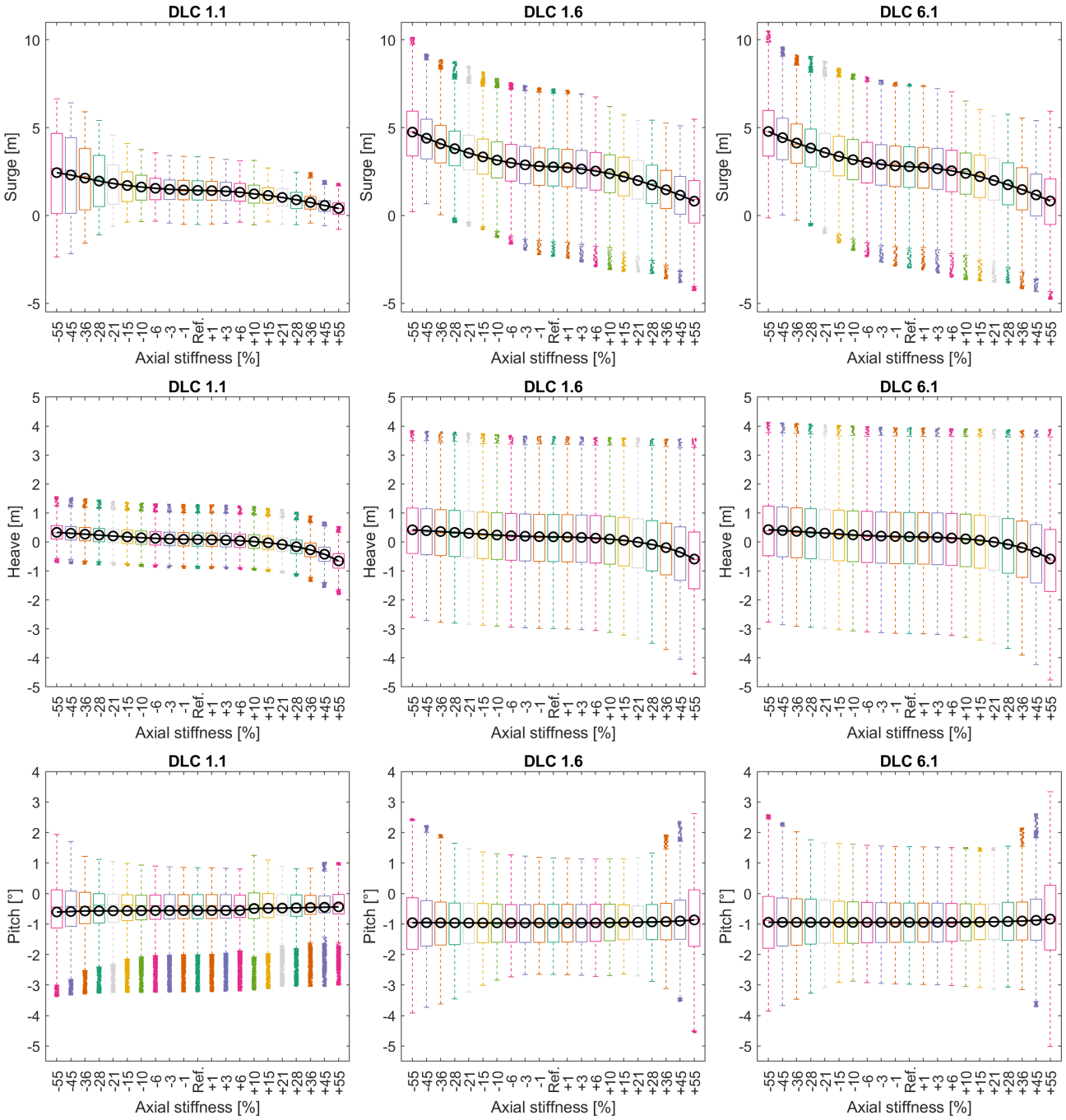

Fig. 7: Statistical comparison of platform displacements in each degree of freedom with different mooring line axial stiffness values in each DLC

The uncertainty between the different axial stiffness and reference stiffness results was assessed in two ways: mean response value and standard deviation of data points. The mean response uncertainty indicates how the mean value of the results changes with varying line axial stiffness, while the standard deviation uncertainty shows how the results are dispersed. Both types of uncertainties were examined, as some results displayed drift with changes in mean value only, while others showed opposite behaviour.

To assess the uncertainty, results of DLC 6.1 were used because it exhibited the highest amplitude values. Axial stiffness values meeting the ±20% uncertainty criteria for each result were superimposed on the load-extension plot, defining the recommended envelope for mooring rope selection. Figure 9 illustrates this visualisation, considering both mean value and standard deviation uncertainty. Notably, choosing a line axial stiffness which achieves ±20% of the reference mean results imposes tighter constraints compared to achieving ±20% of the standard deviation.

IV. Discussion

This design study of a semi-taut mooring system achieved three of the four design requirements. The following section evaluates the mooring system in terms of mitigating platform motion and line tension loads. It also examines the implications for practical tank mooring design.

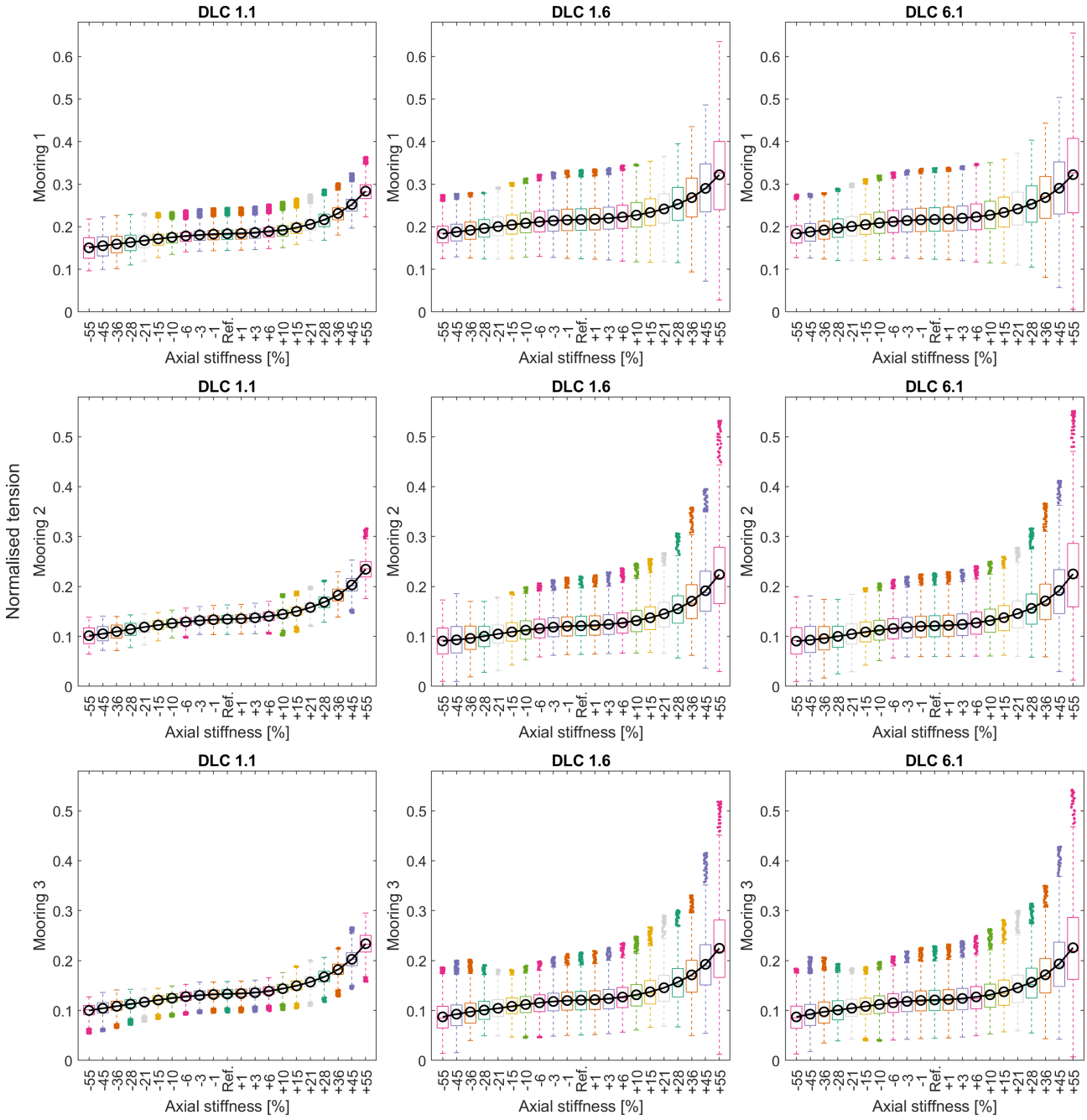

Fig. 8: Comparison of normalised tension in each mooring line with different axial stiffness values in each DLC

A. Limiting platform motion

The surge platform motion peaked at 8.14 m, well below the limit of 25 m. Sway, roll and yaw motion were not considered as are not relevant for aligned environmental conditions. These findings indicate that semi-taut moorings can reliably support electrical cabling technology. Surge was identified as the most sensitive degree of freedom to changes in line stiffness, most prominently under extreme loading conditions. Additionally, it was found that changes in axial stiffness did not impact the standard deviation of surge results.

There was no design limit on the heave response, which was predominately influenced by wave conditions and showed negligible sensitivity to changes in line stiffness. During high-amplitude wave events, such as those in the extreme DLC 6.1, the platform can rapidly drop several meters. These displacements contribute to the peak low tensions observed in mooring lines 2 and 3 due to the reduced effective line length. The sensitivity study indicates that heave results within ±20% of the reference design can be achieved with line axial stiffness values between +6% and -15% of the reference. However, as the heave mean position is near zero, a ±20% change in heave is marginal and so the range of suitable axial stiffness values in reality would be wider. Additionally, changes in line stiffness do not significantly impact the dispersion of heave results.

While not a formal design constraint, the original platform documentation recommended a maximum pitch angle of 6° [23]. The maximum pitch rotation

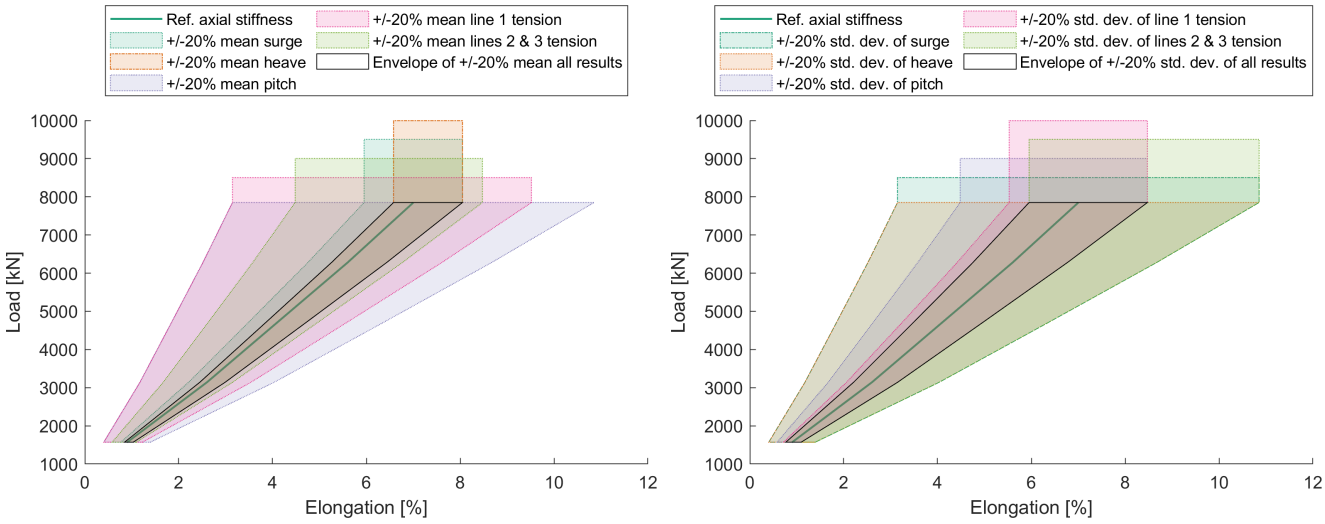

(a) Mean (b) Standard deviation

Fig. 9: Load extension graphs with shaded range of axial stiffness values giving ±20% mean and standard deviation of the reference model's platform motion in each degree of freedom and mooring line tension for DLC 6.1. To note - bands have been extended and stepped vertically to aid visual clarity. This does not represent data obtained from the axial stiffness sensitivity study.

observed in this study was 4.07°. The mean pitch remained unaffected by changes in line axial stiffness across all three DLCs. The lack of relationship between mean pitch rotation and line stiffness suggests that these design parameters are not coupled. This finding may be attributed to the nature of the VolturnUS-S platform which is a semi-submersible type, i.e., it is ballast-stabilised. As a result, the mooring system does not play a significant role in providing the restoring force of the platform in vertical degrees of freedom.

B. Limiting line tension loads

Minimising peak line tension is important to reduce the likelihood and consequences of line failure, resulting in lower investment risk and O&M costs. The design criteria limited the peak tensile load to 60% of the MBL, ensuring a safety factor of 1.67 for a redundant offshore mooring system. Under DLC 6.1, the semi-taut mooring experienced a peak load of 36.8% MBL in line 1, indicating that the design can confidently withstand the conditions of the site. Line 1 had the highest tensile loads due to its alignment with the prevailing environment. The analysis assumed co-linear wind and wave loading, however in reality, conditions can be misaligned, resulting in increased mooring loads [19].

The minimum tensile load was set at 2% MBL to avoid snatch loads which occur when there is a loss of line tension followed by a rapid spike, which can lead to extremely high tensile loads and increase the risk of component failure. In the study, it was observed that the tension in line 3 dropped to 1.7% MBL under DLC 6.1. Albeit a failure of the design criteria, it was deemed acceptable for the purposes of the study.

C. Considerations for tank mooring design

This study developed a functional design of a semi-taut mooring system for the IEA 15 MW RWT and VolturnUS-S platform, aiming to inform a tank test model design. The full-scale mooring system used synthetic rope and marine chain, and for the tank-scale physical model, various representations are possible, such as rope and chain, elastic bungee with a pulley mechanism, or linear/non-linear spring arrangement. The tank-scale axial stiffness can be determined by line material properties or the chosen spring rate, with the option of using extension springs in series or parallel for optimising stiffness. However, this adds complexity to the tank setup, and other factors like maximum extension and loading envelope influence spring selection.

The axial stiffness sensitivity study reveals that values between +6% and −15% of the reference stiffness lead to a maximum ±20% uncertainty in mean dynamic results, expanding to +15% and −21% for uncertainty in the standard deviation of dynamic results. Surge response is likely to have the greatest uncertainty, influencing spring selection based on the expected mooring travel. Contrary to this, another consideration for tank test programs is the realism of numerical model values. Tank testing benefits from realistic hydrodynamic damping and viscous effects, which can be approximated in numerical models, potentially leading to mooring loads lower than numerical equivalents.

A final consideration concerns scaling the mooring geometry. The water depth in this study is 200m. For a typical 1:50th scale model, a tank depth of 4 m would be required. However, many UK-based tank facilities

have shallower depths [41], necessitating a reduction or truncation of the mooring depth for testing purposes.

V. Conclusions

This study successfully designed a typical semi-taut mooring system using synthetic materials suitable for station-keeping of large, future-generation floating offshore wind turbines (FOWT). To develop this mooring proposal, the design requirements of a semi-taut system were first identified and applied to the case study. The platform displacements and mooring line loads demonstrated a strong correlation with the design targets under various loading conditions.

For a conservative analysis, line axial stiffness values ranging from $+6\%$ to -15% of the reference stiffness would yield dynamic results within $\pm 20\%$ of the DLC 6.1 mean reference value. This finding is particularly valuable when selecting mooring line materials for constructing a scaled prototype for tank testing.

A. Recommendations for future work

The next steps in developing this semi-taut mooring design are to investigate misaligned wind and wave conditions, snatch load events, and to simulate the axial stiffness of the synthetic mooring line using hysteresis models. Furthermore, experimental tank testing will be performed to verify and validate the numerical results of both the design of the semi-taut mooring system and the line axial stiffness sensitivity study.

References

[1] M. Harvey *et al.*, "Phase IV Summary Report," 2022.

[2] Equinor, "Hywind Tampen," 2022. [Online]. Available: https://www.equinor.com/energy/hywind-tampen

[3] Principle Power, "Kincardine Offshore Wind Farm," 2022. [Online]. Available: https://www.principlepower.com/projects/kincardine-offshore-wind-farm

[4] Mocean Energy, "Our Technology," 2023. [Online]. Available: https://www.mocean.energy/

[5] AWS Ocean Energy Ltd, "AWS Ocean Energy," 2023. [Online]. Available: https://awsocean.com/

[6] Orbital Marine Power, "Technology," 2023. [Online]. Available: https://www.orbitalmarine.com/

[7] Y. Liu, S. Li, Q. Yi, and D. Chen, "Developments in semi-submersible floating foundations supporting wind turbines: A comprehensive review," *Renewable and Sustainable Energy Reviews*, vol. 60, pp. 433–449, 7 2016.

[8] L. Johanning, P. Theis, and S. Weller, "Technical note: Mooring Testing, MaRINET-D2.21," 2014.

[9] Quoceant Ltd, "High Level Cost Metrics for WEC Machine Elements," 2016.

[10] C. Zhang, S. Wang, S. Xie, J. He, J. Gao, and C. Tian, "Effects of mooring line failure on the dynamic responses of a semisubmersible floating offshore wind turbine including gearbox dynamics analysis," *Ocean Engineering*, vol. 245, p. 110478, 2 2022.

[11] W. West, A. Goupee, S. Hallowell, and A. Viselli, "Development of a Multi-Objective Optimization Tool for Screening Designs of Taut Synthetic Mooring Systems to Minimize Mooring Component Cost and Footprint," *Modelling*, vol. 2, pp. 728–752, 2021.

[12] K. Xu, K. Larsen, Y. Shao, M. Zhang, Z. Gao, and T. Moan, "Design and comparative analysis of alternative mooring systems for floating wind turbines in shallow water with emphasis on ultimate limit state design," *Ocean Engineering*, vol. 219, 1 2021.

[13] M. Ikhennicheu *et al.*, "D2.1 Review of the state of the art of mooring and anchoring designs, technical challenges and identification of relevant DLCs," 2020.

[14] J. Liu and L. Manuel, "Alternative Mooring Systems for a Very Large Offshore Wind Turbine Supported by a Semisubmersible Floating Platform," *Journal of Solar Energy Engineering: Including Wind Energy and Building Energy Conservation*, vol. 140, 2018.

[15] S. Weller, L. Johanning, P. Davies, and S. Banfield, "Synthetic mooring ropes for marine renewable energy applications," *Renewable Energy*, vol. 83, pp. 1268–1278, 2015.

[16] A. Pillai, T. Gordelier, P. Thies, D. Cuthill, and L. Johanning, "Anchor loads for shallow water mooring of a 15 MW floating wind turbine—Part II: Synthetic and novel mooring systems," *Ocean Engineering*, vol. 266, 12 2022.

[17] A. Neisi, H. Ghassemi, M. Iranmanesh, and G. He, "Effect of the multi-segment mooring system by buoy and clump weights on the dynamic motions of the floating platform," *Ocean Engineering*, vol. 260, 9 2022.

[18] S. Verde and E. N. Lages, "A comparison of anchor loads , planar displacement , and rotation for nylon and polyester moored systems for a 15 MW floating wind turbine in shallow water," *Ocean Engineering*, vol. 280, no. May, 2023.

[19] A. Pillai, T. Gordelier, P. Thies, C. Dormenval, B. Wray, R. Parkinson, and L. Johanning, "Anchor loads for shallow water mooring of a 15 MW floating wind turbine — Part I: Chain catenary moorings for single and shared anchor scenarios," *Ocean Engineering*, 7 2022.

[20] F. Papi and A. Bianchini, "Technical challenges in floating offshore wind turbine upscaling: A critical analysis based on the NREL 5 MW and IEA 15 MW Reference Turbines," *Renewable and Sustainable Energy Reviews*, vol. 162, 7 2022.

[21] E. Jump, "Mooring and Anchoring Systems - Market Projections," 2021.

[22] E. Gaertner *et al.*, "Definition of the IEA Wind 15-Megawatt Offshore Reference Wind Turbine," 2020.

[23] C. Allen, A. Viselli, H. Dagher Andrew Goupee, E. Gaertner, N. Abbas, M. Hall, and G. Barter, "Definition of the UMaine VolturnUS-S Reference Platform Developed for the IEA Wind 15-Megawatt Offshore Reference Wind Turbine Technical Report," 2020.

[24] R. Niranjan and S. B. Ramisetti, "Insights from detailed numerical investigation of 15 MW offshore semi-submersible wind turbine using aero-hydro-servo-elastic code," *Ocean Engineering*, vol. 251, 5 2022.

[25] M. de Souza Nascimento, M. Shadman, C. Silva, L. de Freitas Assad, S. Estefen, and L. Landau, "Offshore wind and solar complementarity in Brazil: A theoretical and technical potential assessment," *Energy Conversion and Management*, vol. 270, 2022.

[26] Bridon - Bekaert Ropes, "MoorLine Polyester," 2018.

[27] S. Maxwell, F. Kershaw, C. C. Locke, M. G. Conners, C. Dawson, S. Aylesworth, R. Loomis, and A. F. Johnson, "Potential impacts of floating wind turbine technology for marine species and habitats," *Journal of Environmental Management*, vol. 307, 2022.

[28] M. Borg, M. Collu, and A. Kolios, "Offshore floating vertical axis wind turbines, dynamics modelling state of the art. Part II: Mooring line and structural dynamics," *Renewable and Sustainable Energy Reviews*, vol. 39, pp. 1226–1234, 11 2014.

[29] British Standards Institution, "Stationkeeping systems for floating offshore structures and mobile offshore units BS EN ISO 19901-7:2013," 2013.

[30] American Petroleum Institute, "Design and Analysis of Stationkeeping Systems for Floating Offshore Structures - Draft," 2018.

[31] Det Norske Veritas, "Design of Floating Wind Turbine Structures DNV-OS-J103," 2013.

[32] B. de Miguel Para, "Experimental validation of a floating OWC for wave energy conversion, MARINET - TA1 - MARMOK-A - 1719," Bilbao, 2019.

[33] X. Xu and S. Day, "Experimental investigation on dynamic responses of a spar-type offshore floating wind turbine and its mooring system behaviour," *Ocean Engineering*, vol. 236, 2021.

[34] J. Serret, R. Taylor, M. Yousef, and D. Noble, "DTI-F Scaled model test, MARINET-TA1-DTI-F – DTI-F-14122017," 2018. [Online]. Available: www.marinet2.eu

[35] P. Dafnakis and M. Bonfanti, "Performance evaluation test of a 1:20 scaled ISWEC device in extreme wave conditions, MARINET-TA1-ISWEC 2.0 – 1733," 2018.

[36] Orcina Ltd, "Orcaflex," 2022.

[37] P. Quiggin, "OrcaFlex QA, Testing and Validation Document 99/005:7," 2015.

[38] B. J. Jonkman and M. L. Buhl, "TurbSim User's Guide, NREL/TP-500-39797," 2006.

[39] Det Norske Veritas, "Environmental Conditions and Environmental Loads DNV-RP-C205," 2010.

[40] British Standards Institution, "Wind energy generation systems, Part 3-2: Design requirements for floating offshore wind turbines PD IEC TS 61400-3-2:2019," 2019.

[41] MERiFIC, "Test facilities," 2020. [Online]. Available: https://www.merific.eu/documents/work-package-3-technology-support/3-4-test-facilities/